

## Electronic supplementary information (ESI) for:

# Mapping the role of aromatic amino acids within a blue-light sensing LOV domain

Yonghong Ding,<sup>a,b</sup>Ziyue Zhao,<sup>a</sup>Jörg Matysik,<sup>a</sup> Wolfgang Gärtner<sup>a</sup> and Aba Losi\*<sup>c</sup>

\*: [aba.losi@unipr.it](mailto:aba.losi@unipr.it)

Content:

**Table S1, p. 2:** primers for the variants of *mr4511\_4511*

**Fig. S1, p. 3:** sequence alignment of *Mr4511-C71S* with similar proteins and structural model

**Fig. S2, p. 4:** absorption and fluorescence spectra of *Mr4511* variants

**Fig. S3, p. 5-6:** absorption spectra in the dark and under BL

**Table S2, p. 5:** raw photoacoustics (PA) data for the investigated molecules

**Fig. S4, p. 8:** PA signals for *Mr4511-C71S/Y116W* and Arrhenius plot for the triplet decay

<sup>a</sup>Institute for Analytical Chemistry, University of Leipzig, Linnéstrasse 3, 04103 Leipzig, Germany

<sup>b</sup>Present address: Max Planck Institute for Biophysical Chemistry, Am Fassberg 11, 37077 Göttingen, Germany

<sup>c</sup>Department of Mathematical, Physical and Computer Sciences, University of Parma, Parco Area delle Scienze 7/A, 43124 Parma, Italy. \*: corresponding author, [aba.losi@unipr.it](mailto:aba.losi@unipr.it)

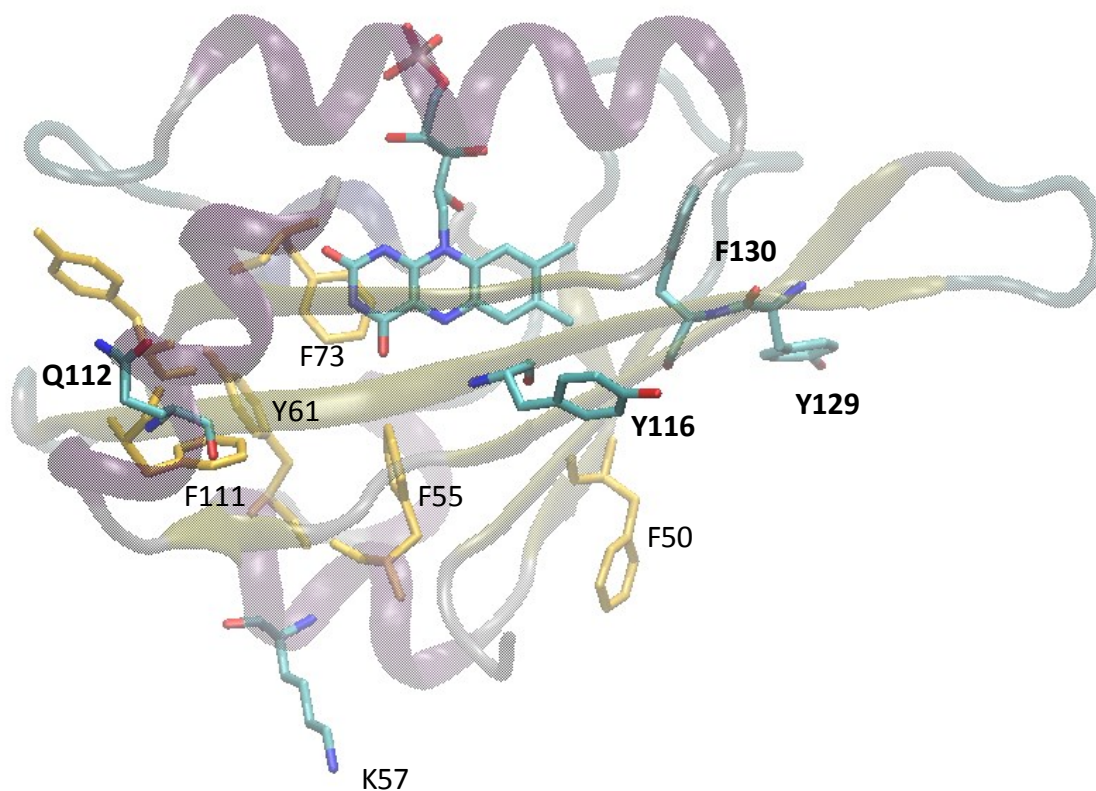
**Table S1.** Primers for the variants of *mrad2831\_4511*. See<sup>1</sup> for C71S and C71S/Q112W

Primer	Sequence (5' to 3')	<b>Mr4511 variants</b>
P1	TGGCTGACCGGCTACACCC	C71S/K57W
P2	CAGGAACGCGTCGTTACGAA	
P3	TTTGTCGGGCCGGTGC	C71S/Y116F
P4	GAGGGCGTTCTGGAAGGTC	
P5	CATGTCGGGCCGGTGC	C71S/Y116H
P6	GAGGGCGTTCTGGAAGGTC	
P7	TGGGTCGGGCCGGTGC	C71S/Y116W
P8	GAGGGCGTTCTGGAAGGTCGAG	
P9	CACTTCTTCGCCTCGCAGCT	C71S/Y129H
P10	GACCACCCGGCCCCGCT	
P11	TGGTTCTTCGCCTCGCAGCT	C71S/Y129W
P12	GACCACCCGGCCCCGCT	
P13	CACTTCGCCTCGCAGCTCGA	C71S/F130H
P14	GTAGACCACCCGGCCCCG	
P15	GTTTCGCCTCGCAGCTCGA	C71S/F130W
P16	CAGTAGACCACCCGGCCCCG	
P17	(same as P15)	F130W
P18	(same as P16)	

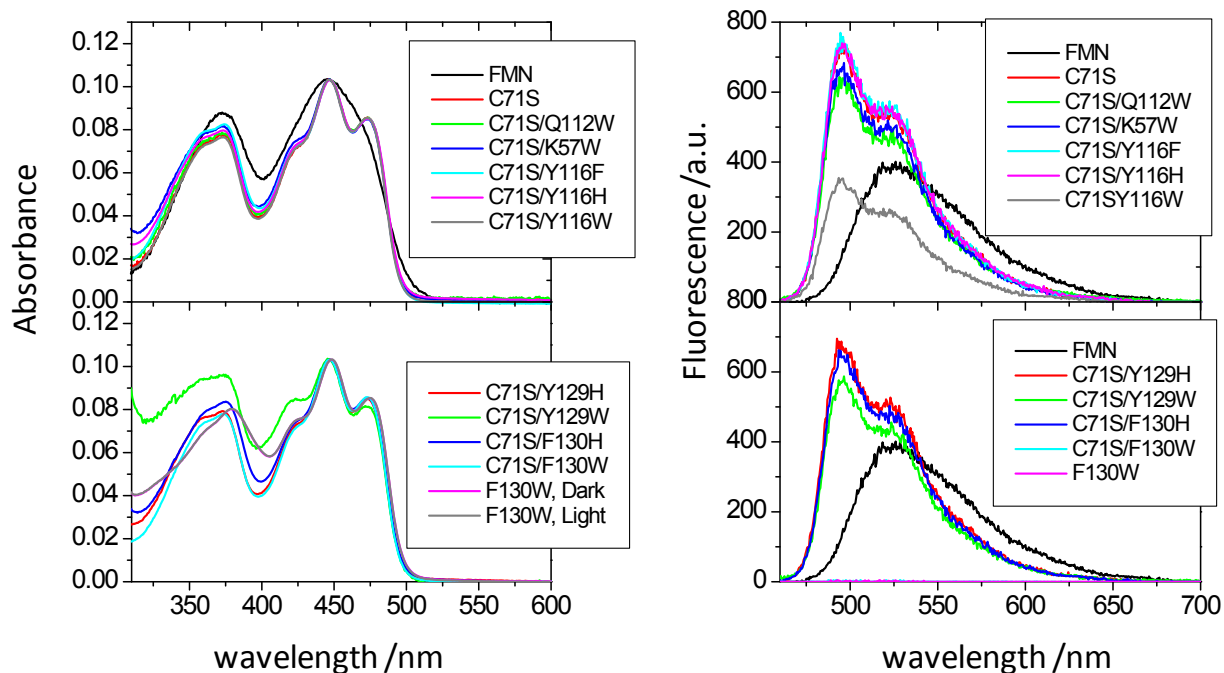
		A $\beta$	B $\beta$	C $\alpha$	D $\alpha$	E $\alpha$	
		. E E E E E E . . . . .	. E E E E E E . . . . .	. H H H H H H . . . . .	. H H H H . . . . .	. H H . . . . .	
		↓ ↓ ↓ ↓ ↓ ↓	↓ ↓ ↓ ↓ ↓ ↓			↓ ↓ ↓ ↓ ↓ ↓	
<i>BsYtvA</i>	25	VGVVITDPALEDNPIVYVNVQGFVQMTGYETEELGKNR				RFLQ	-----
<b>Mr4511-C71S</b>	34	MPMIITDPAQHDNPIVVFVND AFLKLTGYTRMEVVG				RFLQ	-----
<i>Crphot-LOV1</i>	20	HTFVVADATLPCPLVYASEG	F	Y	A	M	T
<i>NcVVD-C108A</i>	71	CALILCDLKQKDTPIVYASEAF	L	Y	M	T	G
<i>AtPHOT2-LOV2</i>	389	KNFVISDPRLPDNPIIFASDS	F	L	E	L	T
<i>iLOV</i>	389	KNFVITDPRLPDNP	I	F	A	S	D
<i>HhBAT</i>	151	IGISISDPLDPYPLVYVND	A	W	R	E	H
			T	G	Y	S	V
			E	E	V	L	G
			R	N	P	R	F
			L	Q			

	F $\alpha$	G $\beta$	H $\beta$	I $\beta$	
	. . . . . H H H H H H H H H H H H . . . . .	. . . . . E E E E E E E E E E . . . . .	. . . . . E E E E E E E E E E E E E E E E . . . . .	. . . . . E E E E E E E E E E E E . . . . .	
	↓ ↓ ↓ ↓ ↓ ↓ ↓ ↓ ↓ ↓	↓ ↓ ↓ ↓ ↓ ↓ ↓ ↓ ↓ ↓	↓ ↓ ↓ ↓ ↓ ↓ ↓ ↓ ↓ ↓	↓ ↓ ↓ ↓ ↓ ↓ ↓ ↓ ↓ ↓	
	GKHTDPAEVDNIR	TALQNKEPVT	VQIQNYKKD	GMTFWNELN	IDPMEI
					--EDKTYFVGIQ
					NDI
					126 O34627
					GPDTAAA
					VDRLRAAIRRE
					DIRVDLLN
					YRKGSTF
					QNALY
					VG
					PVRDEAGR
					VVYF
					FASQLDV
					137 B1M516
					GEGTDPKEV
					QKIRDAIKK
					GEACSV
					RLLN
					YRKGST
					PFWNLL
					TVTP
					IKTPDGR
					VSKFV
					GVQVDV
					123 Q8LPE0
					RKYVDSNT
					INTMRKA
					IDRNAE
					VQVEV
					VNF
					KKG
					QR
					FVNF
					LTMI
					PVRDET
					G
					GEYR
					YS
					SMGF
					QCET
					185 Q1K5Y8
					GPETDQAT
					VQKIRDA
					IRDQRE
					ITVQLIN
					YTKSG
					KKFW
					NLLHL
					QPMRD
					QK
					GELQ
					YF
					IGV
					QLDG
					492 P93025
					GPETDQAT
					VQKIRDA
					IRDQRE
					ITVQLIN
					YTKSG
					KKFW
					NLLHL
					QPMRD
					QK
					GELQ
					YF
					IGV
					QLDG
					492
					GPETDPE
					TVEE
					IAEAI
					GNEE
					EV
					VEI
					IRNY
					RRD
					GT
					PF
					W
					NEL
					TV
					AP
					VY
					DEE
					GLA
					H
					Y
					V
					G
					F
					Q
					NDV
					254 M0FIW0



**Fig. S1.** Top, sequence alignment (performed with the CLUSTAL Omega tool at the European Bioinformatics Institute, EMBL-EBI, using default parameters) of the LOV core of *Mr4511* with other LOV domains mentioned in the text; the secondary structure elements are derived from the structure of *BsYtvA* (PDB access code 2pr5), indicated as E (yellow,  $\beta$ -strands) and H (red,  $\alpha$ -helices). Residues interacting with the chromophore are indicated with arrows. UniProt accession codes are given at the end of each sequence. The site of the reactive cysteine in photosensing LOV domains is shown in white on blue background; mutated residues mentioned in the text are evidenced in cyan; *Bs* = *Bacillus subtilis*; *Nc* = *Neurospora crassa*; *Cr* = *Chlamydomonas reinhardtii*; *At* = *Arabidopsis thaliana*; *Hh* = *Halorubrum hochstenium*. Bottom, structural model of *Mr4511*-LOV (same as in Fig. 2a but 90° rotated); residues labeled in bold have been mutated in this work. Structural modeling was with SWISS-MODEL in the automated mode,<sup>2</sup> rendering with VMD.<sup>3</sup>



**Fig. S2** Left, absorption spectra of the studied proteins; note in the bottom panel that the F130W variant does not show any difference in the absorption spectrum under dark or blue light conditions; right, fluorescence spectra taken at matched absorbance at  $\lambda_{ex}=450$  nm. Besides C71S/F130W and F130W that show negligible fluorescence, the sole variant having a sharply lower fluorescence is C71S/Y116W (top panel). Proteins C71S, C71S/Q112W, C71S/K57W, C71S/Y116W and C71S/F130W were dissolved in buffer NaPi 10 mM, NaCl 100 mM, pH = 8; all other variants in buffer KPi 50 mM, 300 mM NaCl, pH = 8. C71S and C71S/Y116W were studied in both buffers and gave consistent results.

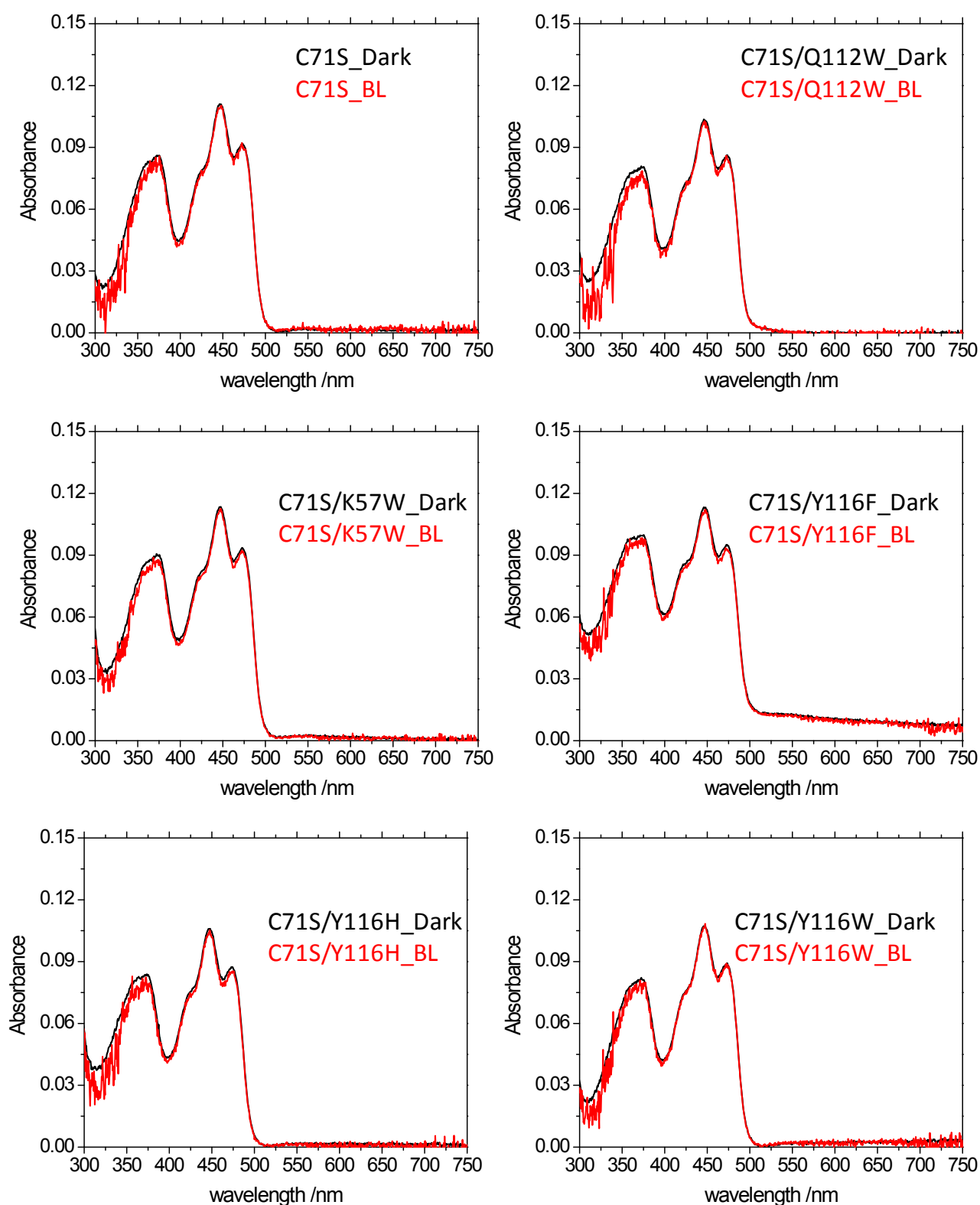


**Fig. S3** (continues next page) Steady state absorption spectra of the investigated *Mr4511* variants investigated in this work in the dark (dark lines) and under BL from LED455 operating at ca. 3 mW; in this latter case 1 ml of sample (at ca. 8  $\mu$ M) was kept illuminated from above the cuvette for the entire duration of the measurement (7 minutes).

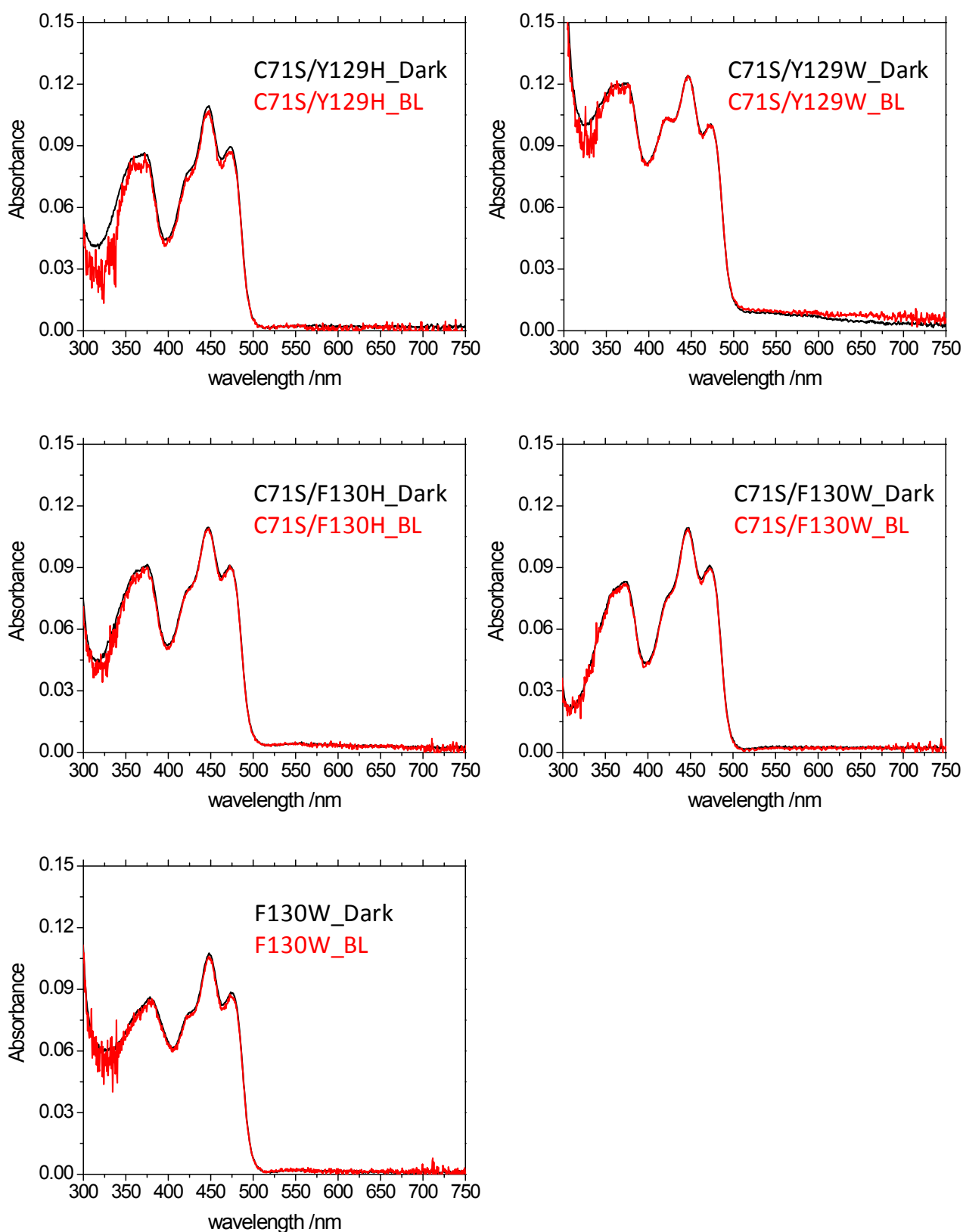
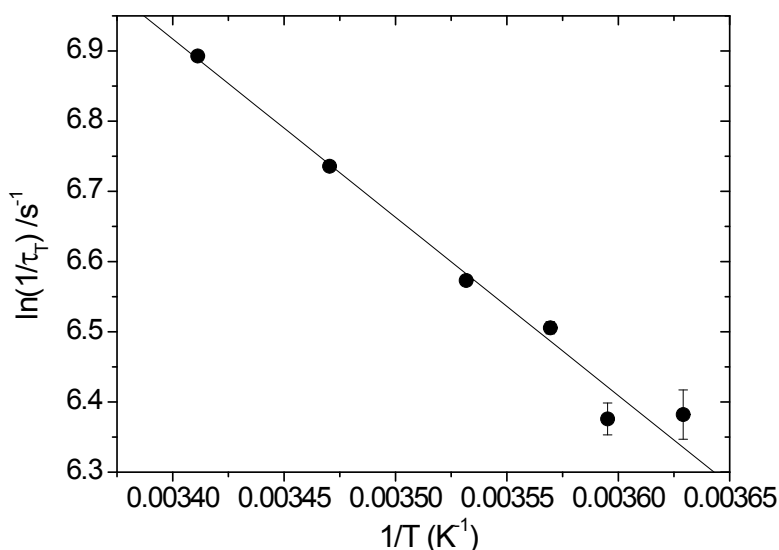
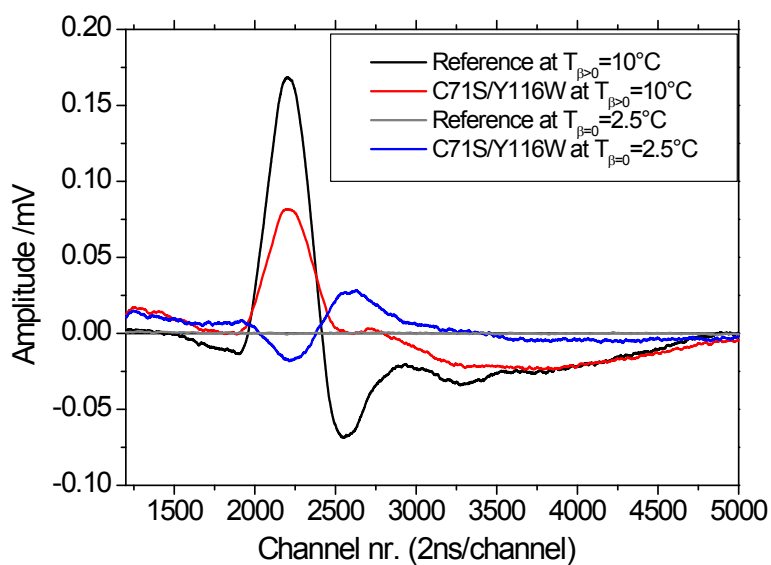


**Fig. S3** (continues from previous page) Steady state absorption spectra of the investigated *Mr4511* variants investigated in this work in the dark (dark lines) and under BL from LED455 (see caption of fig. S2 for details).

**Table S2.** Raw PA data for the investigated proteins and free FMN

Sample	$\alpha_1$ ( $\tau_1 < 20\text{ns}$ )	$\alpha_2$	$\Delta V_1 / \text{ml Einstein}^{-1}$	$\Delta V_2 / \text{ml Einstein}^{-1}$	$\tau_2 / \mu\text{s}$ (20°C)
FMN	$0.40 \pm 0.01$	N.D.	$-1.70 \pm 0.01$	N.D.	$3.5 \pm 0.2$
<b>Mr4511-</b>					
C71S	$0.32 \pm 0.02$	N.D.	$-1.02 \pm 0.02$	N.D.	> 10
C71S/Q112W	$0.30 \pm 0.02$	N.D.	$-0.92 \pm 0.02$	N.D.	> 10
C71S/K57W	$0.30 \pm 0.02$	N.D.	$-0.91 \pm 0.02$	N.D.	> 10
C71S/Y116F	$0.23 \pm 0.02$	N.D.	$-1.33 \pm 0.02$	N.D.	> 10
C71S/Y116H	$0.23 \pm 0.02$	N.D.	$-1.25 \pm 0.02$	N.D.	> 10
C71S/Y116W	$0.44 \pm 0.01$	$0.33 \pm 0.01$	$-1.14 \pm 0.02$	$+2.85 \pm 0.05$	$1.02 \pm 0.05$
C71S/Y129H	$0.28 \pm 0.01$	N.D.	$-1.67 \pm 0.02$	N.D.	> 10
C71S/Y129W	$0.32 \pm 0.02$	N.D.	$-1.15 \pm 0.01$	N.D.	> 10
C71S/F130H	$0.52 \pm 0.02$	N.D.	$-2.27 \pm 0.02$	N.D.	> 10
C71S/F130W	$0.99 \pm 0.02$	N.D.	$\sim 0$	N.D.	N.D.
F130W	$0.97 \pm 0.01$	N.D.	$-0.36 \pm 0.02$	N.D.	N.D.



$$\ln \frac{1}{\tau_T} = -\frac{E_a}{R} \frac{1}{T} + \ln A$$

**Fig. S4.** Top, PA signals at  $T_{\beta=0} = 2.5^\circ\text{C}$  and at  $T_{\beta=0} = 10^\circ\text{C}$  for C71S/Y116W. At  $T_{\beta=0}$  the signal for the reference compound (new coccine) is a zero line; note the shift of the sample signal with respect to the reference, indicative of the resolved kinetics; Bottom, Arrhenius plot for triplet decay in C71S/Y116W, as derived from the deconvolution of PA data between  $3^\circ\text{C}$  and  $20^\circ\text{C}$  ( $\tau_2 = \tau_T$ ). From the linear fit, an activation energy  $E_a = 21\text{ kJ/mol}$  and a pre-exponential factor  $A = 5.7 \times 10^6\text{ s}^{-1}$  was determined.

Note that the signal of the reference ( $H^R$ ) and of the sample ( $H^S$ ) are given by, respectively:<sup>4</sup>

$$H^R = K \left( E_\lambda \frac{\beta}{c_p \rho} \right)$$

and

$$H^S = K \left( Q \frac{\beta}{c_p \rho} + \Delta V \right)$$

where  $E_\lambda$  is the molar excitation energy,  $\beta$  is the volume expansion coefficient,  $c_p$  is the heat capacity at constant pressure, and  $\rho$  is the mass density of the solvent;  $K$  is an instrumental constant. Therefore at  $T_{\beta=0}$ , where heat transport is zero,  $H^R$  vanishes (for the reference all absorbed energy is released as heat within few ps) while  $H^S$  is solely due to volume changes of non thermal origin ( $\Delta V$ ), because the heat  $Q = 0$



- LOV protein yields a singlet oxygen generator, *Photochem. Photobiol. Sci.*, 2019, **18**, 2657–2660.
- 2 M. Biasini, S. Bienert, A. Waterhouse, K. Arnold, G. Studer, T. Schmidt, F. Kiefer, T. Gallo Cassarino, M. Bertoni, L. Bordoli and T. Schwede, SWISS-MODEL: modelling protein tertiary and quaternary structure using evolutionary information., *Nucleic Acids Res.*, 2014, **42**, W252-8.
- 3 W. Humphrey, A. Dalke and K. Schulten, VMD: Visual molecular dynamics, *J. Mol. Graph.*, 1996, **14**, 33–38.
- 4 T. Gensch and C. Viappiani, Time-resolved photothermal methods: accessing time-resolved thermodynamics of photoinduced processes in chemistry and biology, *Photochem. Photobiol. Sci.*, 2003, **2**, 699–721.